

Robust DC-DC Converter Using a-InGaZnO TFTs for Self-Contained Electronics

Bhawna Tiwari*, Pydi Ganga Bahubalindrani**, Mayank Gupta†, Pradeep Mahato†, Deepak†, Ashutosh Tripathi†

Email: bhawnat@iiitd.ac.in ganga@iiserb.ac.in

*Dept. of Electronics and Communication Engineering, IIIT-Delhi, Delhi 110020, India

**Dept. of Electrical Engineering & Computer Science, IISER Bhopal, Bhopal 462066, India

†National Centre for Flexible Electronics, IIT Kanpur, Kalyanpur, Kanpur, Uttar Pradesh 208016, India

Abstract—This paper demonstrates, for the first time, the effect of bias stress on the performance of two amorphous Indium-gallium-Zinc Oxide (a-IGZO) thin-film transistor (TFTs) based DC-DC converters, when they are tested close to real-world operating conditions. The individual circuits (Dickson and Cross-coupled DC-DC converters) are characterized under normal ambient with and without continuous bias stress. Under no stress condition, Dickson and Cross-coupled converters are showing almost constant voltages of 3.8V (8.5V), 3.9V (9.3V), when tested at different clock frequencies of 0.25, 1, 5 MHz with a single (a series of two) thin-film batteries, where each battery shows 3V output voltage. When a Cross-coupled DC-DC converter with 6V input is driving other similar circuit, the final output of 16.5V is noticed, demonstrating self-contained electronics with oxide TFTs. Further, individual circuits were stressed for 18000 seconds to mimic real-world conditions. The Dickson (Cross-coupled) converter has shown a variation of 12% (0.7%) and 5% (0.5%) in output DC voltage when tested with a single and a series connection of two batteries, respectively. This work opens a window for self-contained electronics with oxide TFTs under real-world operating conditions.

Index Terms—Cross-coupled, Dickson, printed batteries, self-contained electronics, stress, oxide TFTs

I. INTRODUCTION

The applications of Amorphous Indium-Gallium-Zinc-Oxide thin-film transistor (a-IGZO TFT) technology are extending into various domains [1]–[5] due to the fabrication of transparent amorphous oxide semiconductor at room temperature [6]. This technology is gaining significant attention in industry and academia due to its unique advantages [7]. However, the technology imposes limitations on circuit design due to the absence of stable and reproducible p-type TFT and non-negligible threshold voltage (V_{TH}) variations with respect to bias stress [8], [9].

Compact self-contained electronics with oxide TFTs are useful for many real-world applications like smart packaging and bio-medical wearable devices, which demand robust on-chip power supply. Though many individual circuits have been reported [10]–[12], the work done towards on-chip power supply generation is very scarce with oxide TFTs. Traditional batteries become bulky for applications under consideration. However, with printing techniques, it is possible to build thin-film batteries, which are light weight. State of art commercially

available thin-film batteries (BV-454523-35ET) are mostly limited to 3V with size approximately 4.5cm x 2cm. In order to obtain the desired on-chip power supply voltage (6V) to drive oxide TFT circuits, DC-DC converters are potential candidate together with printed batteries to ensure compact systems with reasonable active area. Otherwise, a series connection of batteries for on-chip power supply generation would lead to high active area..

DC-DC converter realised using a-IGZO TFTs should deliver almost constant supply voltage continuously for proper operation of the driving circuits. However, due to the charge trapping at the semiconductor/dielectric interface or charge injection into the dielectric in a a-IGZO TFT, shift in V_{TH} has been observed over time [8], [13]. This causes variations in the output DC voltage generated by the converter, and hence, effects the performance of the driving circuits. Though a Cross-coupled converter with diode connected a-IGZO TFTs is demonstrated [14], the characterization is limited to a high input voltage of 10V. Further, the circuit robustness under real-world operating conditions namely under continuous stress, has not been demonstrated. Then this work presents the experimental characterisation of Dickson and Cross-coupled DC-DC converters that can boost the input DC voltage from the thin-film battery/batteries (3 or 6V), when they are under continuous stress. The measured results have demonstrated robustness of the Cross-coupled DC-DC converter, for real-world operating conditions, when compared to the Dickson charge pump. Therefore, from this study, it can be observed that the cross-coupled DC-DC converter is a better selection for on-chip power supply generation (when driven by printed batteries and on-chip clock generation circuits [15]). In addition, its ability to drive other on-chip circuits opens a window for compact self-contained electronics with oxide TFTs in real-world applications.

The rest of the paper is organized as follows: Section II gives details of the fabrication process with measured device characteristics; section III briefly describes the DC-DC converters; Measured results and discussions have been presented in section IV. Finally, conclusions are drawn in section V.

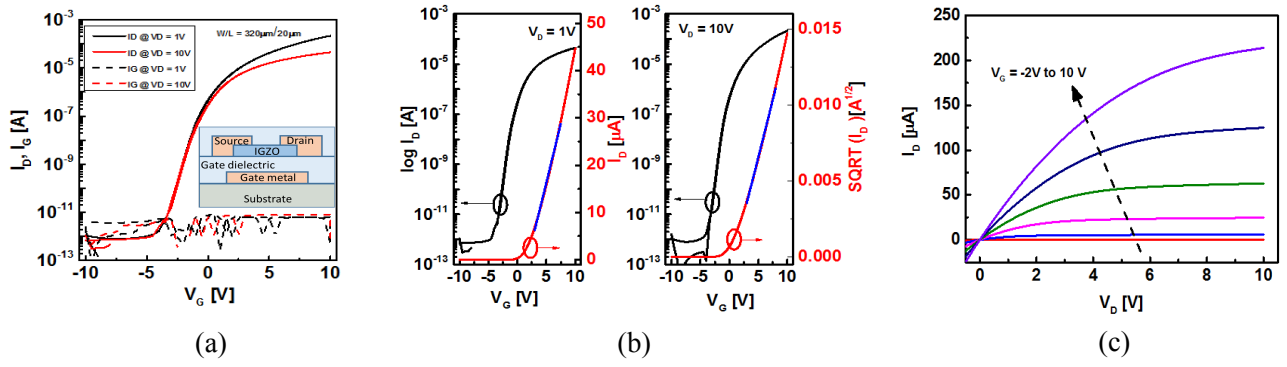


Fig. 1. TFT with $W=320\mu\text{m}$ and $L=20\mu\text{m}$ (a) Transfer characteristics of a TFT in linear ($V_D = 1\text{V}$) and saturation ($V_D = 10\text{V}$) modes. Device cross-sectional schematic is shown in the inset, (b) V_{TH} extraction from transfer characteristics in linear and saturation modes and (c) Output characteristic.

II. A-IGZO TFT: FABRICATION, CHARACTERISTICS AND STRESS MEASUREMENT

TFTs were fabricated on a glass substrate with maximum processing temperature not exceeding 150°C . First, an 80nm thick Mo film was sputtered, and gate electrodes were patterned by photolithography and wet-etching. Subsequently, 80nm thick Al_2O_3 layer was deposited at 150°C using atomic layer deposition. Via holes were opened using standard photolithography and wet-etching. Approximately 25nm thick IGZO film was sputtered from In:Ga:Zn (1:1:1) target under Ar with 2% O_2 at a process pressure of 2mTorr. Semiconductor islands were defined by wet-etching of IGZO film. Approximately 80nm thick Mo source-drain was applied by the lift-off process. Eventually, the whole device was passivated by 80nm thick ALD Al_2O_3 film and subsequently annealed at 150°C for 2 hours on a hotplate under ambient conditions.

I-V characteristics of the TFT were measured using Keithley 4200A-SCS parameter analyzer. Transfer characteristic of a typical TFT are shown in Fig. 1(a) and Fig. 1(b), showing a extracted threshold voltage (V_{TH}) of 1.5V. The output characteristic of the TFT is shown in Fig. 1(c).

As a first step, an isolated TFT (width = $320\mu\text{m}$ and length = $20\mu\text{m}$), is stressed for 3850seconds with gate and drain bias voltages set to -10V and 0V for negative gate bias stress (NBS) and both are set to 10V for positive gate bias stress (PBS). TFT transfer characteristics under PBS and NBS at discrete intervals are shown in Fig. 2(a) and Fig. 2(b), respectively. Variations in V_{TH} with stress duration is shown in Fig. 2(c). A positive shift of around 0.73V in V_{TH} of the TFT can be observed after 3850 seconds, which is possibly due to the charge trapping at the semiconductor/dielectric interface or charge injection into the dielectric [8], [13]. On the other hand, a negative shift of around 0.54V has been observed. The shift is due to positively charged donor-like sub-gap density of states, which provides additional carriers for conduction [13]. The shift in V_{TH} due to bias stress, impacts the circuit performance under real-world conditions, which demands continuous operation, mainly when the output voltage is a function of V_{TH} .

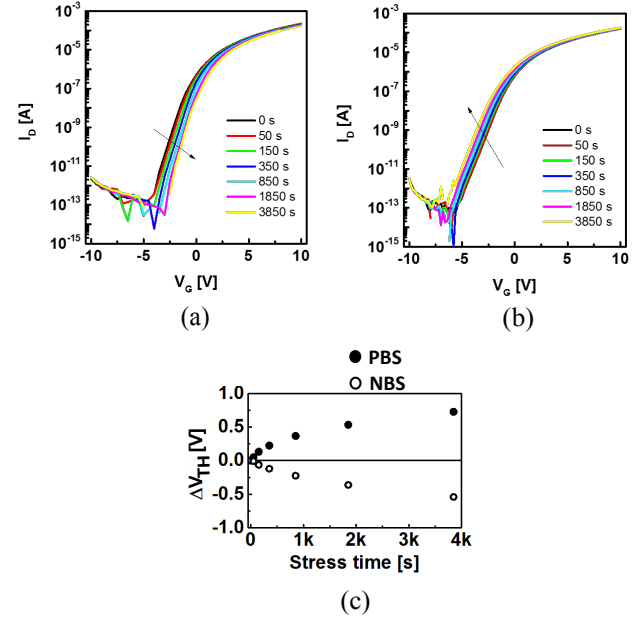


Fig. 2. TFT with $W=320\mu\text{m}$ and $L=20\mu\text{m}$ (a) PBS. Stress conditions were set as $V_G = V_D = 10\text{V}$ (b) NBS. Stress conditions were set as $V_G = -10\text{V}$, $V_D = 0\text{V}$ and (c) Threshold voltage shift with time for PBS (solid symbols) and NBS (open symbols).

III. IMPACT OF STRESS ON THE PERFORMANCE OF DC-DC CONVERTER

Circuit schematics and micro-graphs of Dickson and Cross-coupled DC-DC converters using IGZO TFTs are presented in Fig. 3. Here, clk and $clkb$ are non-overlapping clock pulses which oscillates between 0V and supply voltage (V_{DD}).

A. Dickson Converter

In Dickson converter (Fig. 3(a)), when clk is at 0V, M_1 is ON and the top plate of C_1 charges towards V_{DD} . Since M_1 has a diode connection, there is a V_{TH} drop and the voltage at node V_1 settles to $V_{DD} - V_{TH}$. On the other hand when clk is at V_{DD} , M_2 turns ON and clk voltage will be in series with V_1 and V_{OUT} becomes $2(V_{DD} - V_{TH})$. Unless there is

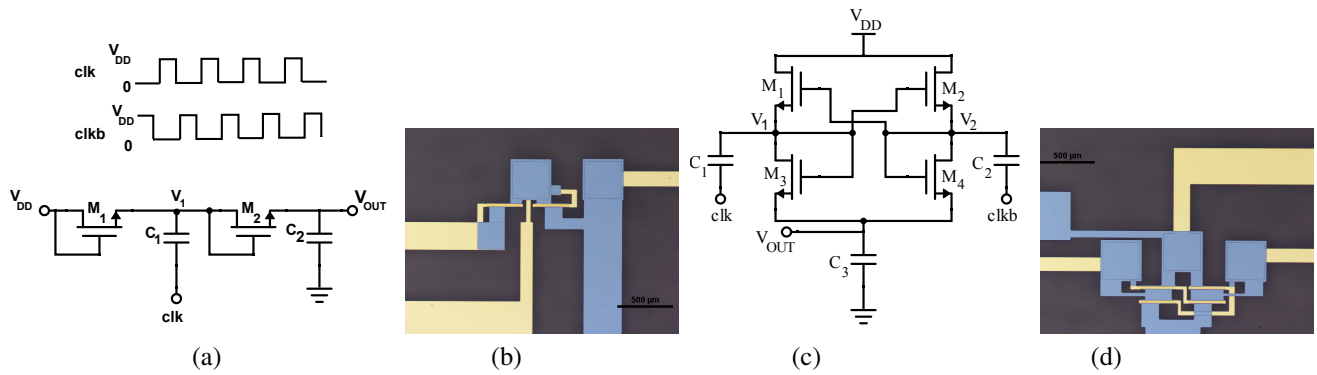


Fig. 3. DC-DC converters (Charge pump) using a-IGZO TFTs (a) Circuit schematic of Dickson (b) Micro-graph of Dickson (c) Circuit schematic of Cross-coupled and (d) Micro-graph of Cross-coupled configurations.

a leaky path, this voltage can be maintained. Since V_{OUT} is a direct function of V_{TH} , it shows variations with bias stress.

B. Cross-coupled Converter

In the Cross-coupled DC-DC converter (see Fig. 3(c)), when clk is at 0V and $clkb$ is at V_{DD} , V_1 charges towards V_{DD} through M_1 . At the same time M_3 and M_2 are OFF and voltage at node V_2 is $2V_{DD}$, assuming V_2 is raised to V_{DD} by M_2 when clk is at V_{DD} and $clkb$ is at 0V. Therefore, V_{OUT} settles at $2V_{DD} - V_{TH}$ through M_4 .

Unlike Dickson, this converter has one V_{TH} drop less at the output. Besides, during operation, V_1 (V_2) oscillates between V_{DD} and $2V_{DD}$ when clk ($clkb$) is 0V and V_{DD} , respectively, which prevents continuous turning ON of all the transistors due to cross-coupling action. While only M_2 and M_3 are ON when clk is V_{DD} , only M_1 and M_4 are ON when $clkb$ is V_{DD} . Therefore, the Cross-coupled converter is expected to show better performance under stress when compared to Dickson.

IV. RESULTS AND DISCUSSIONS

All the measurements were carried out at normal ambient. It should be noted that for testing the converters in real-world environment, the supply voltage (V_{DD}) is generated externally, using thin-film printed batteries. Circuit test setup with a series connection of two thin-film printed batteries, and measured response of Cross-coupled circuit is shown in Fig. 4(a). The response of the circuits at different clk frequencies (250KHz, 1MHz, and 5MHz) is shown in Fig. 4(b) when they are tested with a single and series connection of two thin-film batteries. As expected, both circuits are not showing variations in the output voltage with respect to clock frequencies. The Cross-coupled circuit is showing slightly improved response as the overdrive voltage drop is lower than the threshold voltage drop due to the absence of diode connections. From simulations and for a load current of $100\mu A$, the Cross-coupled converter has shown a power efficiency (η) of 79.54% compared to Dickson where it is 72.10%. The lower efficiency of Dickson converter is due to the extra V_{TH} drop of diode connected transistors.

When a TFT is stressed for 3850 seconds, nearly 48% increase in V_{TH} has been observed (see Fig.1(c)). Both Dickson

and Cross-coupled DC-DC converters response with respect to stress is being presented in Fig. 4(c). The Dickson converter has shown a 5% (6V supply) and 12% (3V supply) drop in the output DC voltage compared to Cross-coupled, where the drop is as low as 0.5% (6V supply) and 0.7% (3V supply) after 18000 seconds of stress. Since V_{TH} is becoming positive with respect to stress, Dickson charge pump performance is being degraded as expected. On the other hand, Cross-coupled circuit is showing almost robust performance against stress as explained in previous section. It should be noted that the robust performance of the cross-coupled converter is due its cross-coupling circuit architecture (explained previously) and a similar performance can be expected when a non-rigid (flexible) substrates are used.

In order to obtain higher DC voltages and test the driving capability of the converters (to drive other circuits in a self-contained system), two DC-DC converters are cascaded. The test setup and measured response are shown in Fig. 4(d). The measured DC voltages with different combination of the converters are summarised in Table I. In addition, the table also presents value of η for each case, which has been calculated for $100\mu A$ load current. Expected results are observed from the table when DC-DC Converter-2 (see Fig. 4(d)) is a Cross-coupled converter as the cross-coupling action isolates V_{OUT1} from the load at V_{OUT2} , thus, ensures higher output DC voltage. However, if the Dickson converter is used, V_{OUT1} is degraded, which reduces V_{OUT2} .

TABLE I
RESPONSE OF CASCADED DC-DC CONVERTERS.

DC-DC Converter-1	DC-DC Converter-2	V_{OUT1} (V)	V_{OUT2} (V)	η (%)
Dickson	Dickson	7.5	12	66.5
Dickson	Cross-coupled	8.4	13.5	72.23
Cross-coupled	Dickson	8.8	13	69.13
Cross-coupled	Cross-coupled	9.2	16.5	83

V. CONCLUSIONS

This work presents the experimental characterization of two DC-DC converters namely, Dickson and Cross-coupled, using

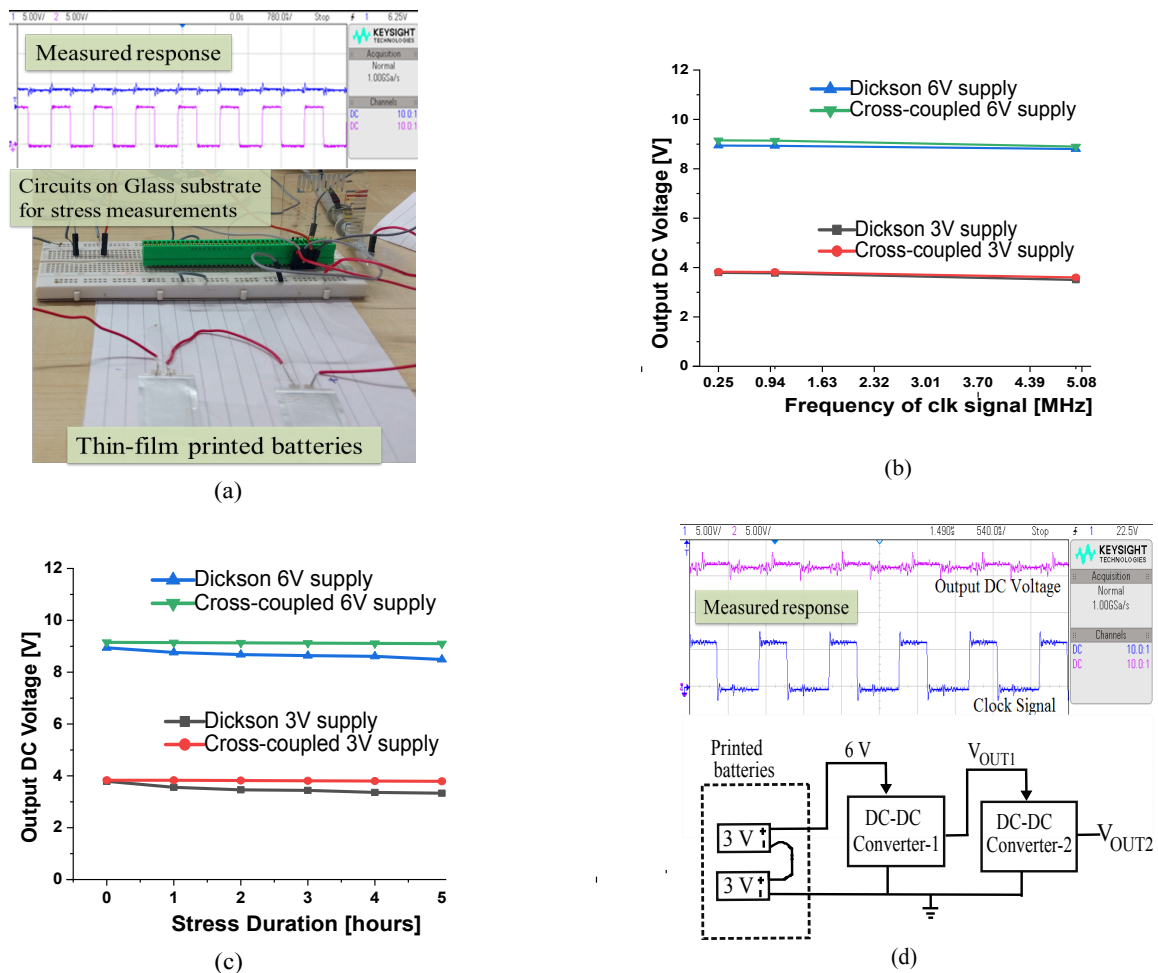


Fig. 4. (a) Test setup for stress measurements using thin-film printed batteries with measured response of Cross-coupled converter, (b) Measured response at different clk frequencies, (c) Measured response against bias stress and (d) Test setup for cascaded DC-DC converters with measured response of Cross-coupled driving Cross-coupled converter.

a-IGZO TFTs under bias stress. In order to test the suitability of the circuits for self-contained electronics, the circuits are tested, for the first time, close to real-world condition by stressing them for 18000 seconds using printed batteries. The measurement result has shown a robust performance of Cross-coupled converter compared to Dickson charge pump. Hence, this study enables realisation of compact self-contained electronics with oxide TFTs for many real-world applications including smart packaging, biomedical wearable devices, NFC and RFIDs.

ACKNOWLEDGMENT

This work is partly supported by early career research grant with project ref. ECR/2017/000931 and IISER Bhopal. This work is also supported by Ministry of Electronics Information Technology, Government of India, grant for the Centre of Excellence for Large Area Flexible Electronics (Project ref. 2(4)/2014-PEGD(IPHW)). The publication is also an outcome of the R & D work under-taken under the Visvesvaraya PhD Scheme of Ministry of Electronics Information Technology, being implemented by Digital India Corporation.

REFERENCES

- [1] S. H. Cho, S. W. Kim, W. S. Cheong, C. W. Byun, C.-S. Hwang, K. I. Cho, and B. S. Bae, "Oxide thin film transistor circuits for transparent RFID applications," *IEICE transactions on electronics*, vol. 93, no. 10, pp. 1504–1510, 2010.
- [2] A. Chasin, V. Volskiy, M. Libois, K. Myny, M. Nag, M. Rockel , G. A. Vandenbosch, J. Genoe, G. Gielen, and P. Heremans, "An integrated a-IGZO UHF energy harvester for passive RFID tags," *IEEE Transactions on Electron Devices*, vol. 61, no. 9, pp. 3289–3295, 2014. [Online]. Available: doi: 0.1109/TED.2014.2340462
- [3] Y. Chen, D. Geng, and J. Jang, "P-24: Integrated Gate Driver for 2700-ppi 8K 120Hz Displays using a-IGZO TFTs," in *SID Symposium Digest of Technical Papers*, vol. 49, no. 1. Wiley Online Library, 2018, pp. 1268–1271. [Online]. Available: https://doi.org/10.1002/sdtp.12144
- [4] S. Shah, J. Smith, J. Stowell, and J. B. Christen, "Biosensing platform on a flexible substrate," *Sensors and Actuators B: Chemical*, vol. 210, pp. 197–203, 2015. [Online]. Available: https://doi.org/10.1016/j.snb.2014.12.075
- [5] A. K. Tripathi, K. Myny, B. Hou, K. Wezenberg, and G. H. Gelinck, "Electrical characterization of flexible InGaZnO transistors and 8-b transponder chip down to a bending radius of 2 mm," *IEEE Transactions on Electron Devices*, vol. 62, no. 12, pp. 4063–4068, Dec 2015. [Online]. Available: 10.1109/TED.2015.2494694
- [6] K. Nomura, H. Ohta, A. Takagi, T. Kamiya, M. Hirano, and H. Hosono, "Room-temperature fabrication of transparent flexible thin-film transistors using amorphous oxide semiconductors," *Nature*,

vol. 432, no. 7016, pp. 488–492, Oct 2004. [Online]. Available: <https://doi.org/10.1038/nature03090>

- [7] T. Kamiya, K. Nomura, and H. Hosono, “Present status of amorphous In–Ga–Zn–O thin-film transistors,” *Science and Technology of Advanced Materials*, vol. 11, no. 4, p. 044305, 2010. [Online]. Available: doi:10.1088/1468-6996/11/4/044305
- [8] J. Martins, P. Bahubalindruni, A. Rovisco, A. Kiazadeh, R. Martins, E. Fortunato, and P. Barquinha, “Bias stress and temperature impact on InGaZnO TFTs and circuits,” *Materials*, vol. 10, no. 6, p. 680, 2017. [Online]. Available: doi:10.3390/ma10060680
- [9] D. Wang, W. Zhao, H. Li, and M. Furuta, “Drain Current Stress-Induced Instability in Amorphous InGaZnO Thin-Film Transistors with Different Active Layer Thicknesses,” *Materials*, vol. 11, no. 4, p. 559, 2018. [Online]. Available: doi:10.3390/ma11040559
- [10] P. G. Bahubalindruni, V. G. Tavares, J. Borme, P. G. de Oliveira, R. Martins, E. Fortunato, and P. Barquinha, “InGaZnO Thin-Film-Transistor-Based Four-Quadrant High-Gain Analog Multiplier on Glass,” *IEEE Electron Device Letters*, vol. 37, no. 4, pp. 419–421, April 2016. [Online]. Available: doi:10.1109/LED.2016.2535469
- [11] P. G. Bahubalindruni, J. Martins, A. Santa, V. Tavares, R. Martins, E. Fortunato, and P. Barquinha, “High-gain transimpedance amplifier for flexible radiation dosimetry using InGaZnO TFTs,” *IEEE Journal of the Electron Devices Society*, vol. 6, pp. 760–765, 2018. [Online]. Available: doi:10.1109/JEDS.2018.2850219
- [12] N. P. Papadopoulos, F. De Roose, J.-L. P. van der Steen, E. C. Smits, M. Ameys, W. Dehaene, J. Genoe, and K. Myny, “Toward Temperature Tracking With Unipolar Metal-Oxide Thin-Film SAR C-2C ADC on Plastic,” *IEEE Journal of Solid-State Circuits*, 2018. [Online]. Available: doi: 10.1109/JSSC.2018.2831211
- [13] E. N. Cho, J. H. Kang, C. E. Kim, P. Moon, and I. Yun, “Analysis of bias stress instability in amorphous ingazno thin-film transistors,” *IEEE Transactions on Device and Materials Reliability*, vol. 11, no. 1, pp. 112–117, March 2011. [Online]. Available: 10.1109/TDMR.2010.2096508
- [14] S.-H. Hong, I.-S. Yang, J.-S. Kang, T.-H. Hwang, O.-K. Kwon, C.-W. Byun, W.-S. Cheong, C.-S. Hwang, and K.-I. Cho, “DC–DC converters using indium gallium zinc oxide thin film transistors for mobile display applications,” *Japanese Journal of Applied Physics*, vol. 49, no. 3, p. 03CB05, mar 2010. [Online]. Available: <https://doi.org/10.1143%2Fjjap.49.03cb05>
- [15] B. Tiwari, J. Martins, S. Kalla, S. Kaushik, A. Santa, P. G. Bahubalindruni, V. G. Tavares, and P. Barquinha, “A high speed programmable ring oscillator using ingazno thin-film transistors,” in *2018 International Flexible Electronics Technology Conference (IFETC)*, Aug 2018, pp. 1–6. [Online]. Available: 10.1109/IFETC.2018.8584006